Redox Biology 47 (2021) 102147

Contents lists available at ScienceDirect

Redox Biology

journal homepage: www.elsevier.com/locate/redox

Endothelial peroxynitrite causes disturbance of neuronal oscillations by targeting caspase-1 in the arcuate nucleus

Meiling Sun [a,1], Xing-Feng Mao [a,1], Zheng-Mao Li [a,1], Zhi-Hui Zhu [a], Dong-Mei Gong [b], Lu Lu [a], Xiang Chen [a], Yu Zhang [a], Kohji Fukunaga [c], Yong Ji [a,d], Ai-Hua Gu [e,**], Ying-Mei Lu [b,f,*], Feng Han [a,d,f,***]

[a] Key Laboratory of Cardiovascular & Cerebrovascular Medicine, Drug Target and Drug Discovery Center, School of Pharmacy, Nanjing Medical University, Nanjing 211166, China
[b] Department of Physiology, Nanjing Medical University, Nanjing 211166, China
[c] Department of Pharmacology, Graduate School of Pharmaceutical Sciences, Tohoku University, Sendai 980-8578, Japan
[d] Gusu School, Nanjing Medical University, Suzhou Municipal Hospital, The Affiliated Suzhou Hospital of Nanjing Medical University, Suzhou 215000, China
[e] State Key Laboratory of Reproductive Medicine, Institute of Toxicology, School of Public Health, Nanjing Medical University, Nanjing 211166, China
[f] Institute of Brain Science, The Affiliated Brain Hospital of Nanjing Medical University, Nanjing 211166, China

ARTICLE INFO

Keywords:
Cisplatin
Peroxynitrite
Caspase-1
Neuronal oscillations
Arcuate nucleus

ABSTRACT

Severe anorexia limits the clinical application of cisplatin, and even leads to the discontinuation of treatment. However, the mechanisms underlying cisplatin-induced anorexia are unknown. Herein, we demonstrated that cisplatin could affect neuronal gamma oscillations and induce abnormal neuronal theta-gamma phase-amplitude coupling in the arcuate nucleus (Arc) of the hypothalamus, and these findings were associated with significantly decreased food intake and weight loss in mice. Chemogenetic activation of AgRP neurons in the Arc reversed the cisplatin-induced food intake reduction in mice. We further demonstrated that endothelial peroxynitrite ($ONOO^-$) formation in the Arc induced nitrosative stress following cisplatin treatment via a previously uncharacterized pathway involving neuronal caspase-1 activation. Strikingly, treatment with the $ONOO^-$ scavenger uric acid (UA) reversed the reduced action potential (AP) frequency of AgRP neurons and increased the AP frequency of POMC neurons induced by SIN1, a donor of $ONOO^-$, in the Arc, as determined by whole-cell patch-clamp electrophysiological recording. Consistent with these findings, UA treatment effectively alleviated cisplatin-induced dysfunction of neuronal oscillations and neuronal theta-gamma phase-amplitude coupling in the Arc of mice. Taken together, these results suggest, for the first time, that targeting the overproduction of endothelial $ONOO^-$ can regulate cisplatin-induced neurotoxicity through neuronal caspase-1, and thereby serve as a potential therapeutic approach to alleviate chemotherapy-induced anorexia and weight loss.

1. Introduction

Cisplatin (*cis*-diamminedichloroplatinum II) is one of the most widely used chemotherapeutic agents for treating malignant tumors in the clinic [1]. Unfortunately, the therapeutic efficacy of cisplatin is limited by its dose- and time-dependent side effects [2]. Nausea, emesis, anorexia and weight loss, present in approximately 80% of cancer patients receiving cisplatin treatment, are the most common side effects of cisplatin, and these side effects decrease the quality of life and survival of cancer patients [3]. Although several clinical approaches have been developed to prevent nausea and emesis (e.g., 5-hydroxytryptamine receptor antagonists, neurokinin-1 antagonists, dexamethasone and olanzapine), they lead to other side effects, such as headache and severe gastrointestinal dysfunction, especially in the later phases of chemotherapy [4]. Furthermore, a cumulative cisplatin dose of 350

* Corresponding author. Department of Physiology, Nanjing Medical University, Nanjing 211166, China.
** Corresponding author. State Key Laboratory of Reproductive Medicine, Institute of Toxicology, School of Public Health, Nanjing Medical University, Nanjing 211166, China.
*** Corresponding author. Key Laboratory of Cardiovascular & Cerebrovascular Medicine, Drug Target and Drug Discovery Center, School of Pharmacy, Nanjing Medical University, Nanjing 211166, China.
E-mail addresses: aihuagu@njmu.edu.cn (A.-H. Gu), lufx@njmu.edu.cn (Y.-M. Lu), fenghan169@njmu.edu.cn (F. Han).
[1] The first three authors contributed equally to this study.

https://doi.org/10.1016/j.redox.2021.102147
Received 13 August 2021; Received in revised form 13 September 2021; Accepted 20 September 2021
Available online 27 September 2021

Abbreviations

AHP	afterhyperpolarization
AP	action potential
Arc	arcuate nucleus
AgRP	agouti-related protein
Casp1	caspase-1
CFC	cross-frequency coupling
CNO	clozapine-N-oxide
GO	gene ontology
HBMECs	human brain microvascular endothelial cells
LFP	local field potential
LPS	lipopolysaccharide
MI	modulation index
$NO^{\bullet}$	nitric oxide
NPY	neuropeptide
$O_2^{\bullet-}$	superoxide
$ONOO^-$	peroxynitrite
POMC	proopiomelanocortin
RMP	resting membrane potential
SIN1	3-Morpholinosydnonimine
UA	uric acid

mg/m^2 has been considered as the threshold values for neurotoxicity development [5]. Nonetheless, the exact mechanism of cisplatin-induced feeding behavior disorder remains to be elucidated, and there is no effective prevention for the side effects of cisplatin [6].

It is well documented that, within the central nervous system, hypothalamic nuclei is involved in the regulation of feeding and energy expenditure, such as the arcuate nucleus (Arc), the lateral hypothalamic area and the dorsomedial nucleus [7–9]. The Arc is critical for feeding behavior and body weight regulation. The Arc is located adjacent to the third ventricle and has a weak or modified blood-brain barrier, which ensures vulnerability to damage induced by circulating toxins or metabolites [10,11]. Numerous studies demonstrate that there are two classes of peptide-producing neurons in the Arc, with each class exerting distinct opposing actions on feeding: orexigenic neurons which produce agouti-related protein (AgRP) and neuropeptide (NPY) to promote food intake, while anorexigenic neurons which express proopiomelanocortin (POMC) to inhibit feeding behavior [12,13]. Feeding behavior is suppressed when the function of AgRP neurons is blocked and POMC neurons are activated [14]. However, the mechanisms underlying cisplatin-induced neurotoxicity associated with the Arc neurons in the hypothalamus remain unclear.

Persistent inflammation and oxidative/nitrosative stress have been shown to play causative roles during platinum-based chemotherapy [15]. The associated toxic amounts of reactive oxygen/nitrogen species (ROS/RNS) lead to a cellular apoptotic cascade via NLRP3 inflammasome activation [16,17]. Cisplatin induces ototoxicity and nephrotoxicity through caspase-1 activation [18,19]. Activated caspase-1 promotes the maturation and secretion of proinflammatory cytokines, such as IL-1β and IL-18 [20]. Caspase-1 gene ablation or pharmacological intervention protected against cisplatin-induced acute kidney injury [18,21]. The generation of peroxynitrite ($ONOO^-$) and nitrosative stress was also reported to participate in cisplatin-induced damage in the kidney and ototoxicity [22–24]. However, it is unclear whether inflammation and $ONOO^-$ are involved in the neurotoxicity induced by cisplatin, and the mechanism underlying this neurotoxicity remains to be clarified.

Here, we provide direct evidence of abnormal neuronal gamma oscillations and neuronal theta-gamma phase-amplitude coupling in the Arc after cisplatin exposure. Notably, endothelial $ONOO^-$ generation by cisplatin mediates neuronal caspase-1 activation, which induces abnormal neuronal action potential in the Arc. We further show that an $ONOO^-$ scavenger (UA) can eliminate cisplatin-induced neurotoxicity and consequently alleviate the feeding behavior disorder associated with cisplatin-based chemotherapy.

2. Methods and materials

2.1. Animals

Male C57BL/6J mice (9–11 weeks old) were purchased from SLAC-CAL Lab Animal Ltd. (Shanghai, China) and used in this study. *Agrp-cre* mice (The Jaxson Lab, Stock No: 012899) were the gift from Professor Zhan at the National Institute of Biological Science (NIBS). *Agrp-cre*; Ai 14 mice were obtained by crossing *Agrp-cre* mice with Ai14 mice (Rosa26-tdTomato Cre reporter line, Stock No: 007914, The Jackson Laboratory). Caspase-1-deficient mice ($Casp1^{-/-}$) were the gift from Professor Lu at Nanjing Medical University (NJMU). All mice were bred in house and were allowed water and food *ad libitum*. Housing was kept constant at 22 ± 2 °C, and a 12/12 h reverse dark-light cycle was employed. All experimental procedures were carried out in accordance with protocols submitted to and approved by the Nanjing Medical University Institutional Animal Care and Use Committee.

2.2. Cisplatin treatment procedure

For the acute phase, mice were administered intraperitoneally (i.p.) with cisplatin (P4394 Sigma, USA) at the dose of 6 mg/kg and used for further experiments. Body weight and food consumption were assessed at 24 h after cisplatin treatment. For the chronic phase, wide-type (WT) mice or $Casp1^{-/-}$ mice were daily treated with cisplatin (2.3 mg/kg, i.p.) or saline for 5 days, and then rested for 5 days, followed by another 5 days injection and 5 days rest according to the procedure in clinic [25]. Total cumulative doses of 23 mg/kg cisplatin were used for mice which approximating human therapeutic doses relative to body weight. Body weights were measured daily at the time of cisplatin injections. In accordance with the Institution Animal Care and Use Committee of Nanjing Medical University, the mice were removed and humanely euthanized when a weight loss was more than 20–25%. The weight change from baseline (Day 1) was calculated. Food intake was calculated as the difference between the food provided initially and the unconsumed food.

2.3. Drug administration

To investigate the effects of UA (216–00222, Wako, Japan) on the neurotoxicity induced by cisplatin, mice were randomly assigned to pretreat with UA (250 mg/kg, i.p.) for 3 days prior to cisplatin administration. Then, UA was administered everyday continuously for another 20 consecutive days at 6 h before the cisplatin injection.

To discuss the role of caspase-1 involved in the food intake disrupted by cisplatin, mice were pretreated with the caspase-1 inhibitor VX-765 (Belnacasan, S2228, Selleck, 100 mg/kg, i.v.) before cisplatin administration for 1 h. Food intake and weight of mice were measured at 24 h after cisplatin treatment.

2.4. Surgery for implantation of tetrodes

Mice were deeply anesthetized and mounted in a stereotactic apparatus. Then, the fur on the surface of the scalp was removed and a hole was drilled above the right arcuate nucleus for implantation (Arc from bregma: antero-posterior, −1.58 mm; medio-lateral, 0.2 mm). For local field potential (LFP) recording, the tetrodes were implanted into the Arc. They were lowered to an average depth between 5.6 and 5.8 mm to target the Arc. Each tetrode consists of eight polyimide-coated nichrome wires (single-wire diameter, item no. PF000591. RO-800, 0.0005" 12.7 μm, coating 1/4 hard PAC, Sandvik) connected to a 32-channel

electrode interface board (EIB-32, Neuralynx). Skull screws overlying the cerebellum and frontal cortex served as ground and reference, respectively. Finally, the tetrodes were sealed to the bone by dental acrylic. A custom-made aluminum head plate was attached to the skull with stainless steel screws and dental cement. After surgery, mice were housed individually for further experiments.

2.5. Local field potential recordings

Recordings were made during tetrodes implantation to ensure optimal placement within Arc. The signals recorded from the tetrodes were sent to a headstage and amplified by a 32-channel amplifier, and then were sampled at 20 kHz by a Neuralynx recording system. For LFP recordings, after recovered from surgery for at least 1 week, the awake mice were placed in home cages during spontaneous behavior before or after cisplatin treatment. LFP signals were amplified (1000 × gain, Neuralynx), filtered at 0.1–250 Hz, and sampled at 1 kHz. LFP signals were recorded via the same Neuralynx recording system.

2.6. Spectral analysis and phase-amplitude coupling

Spectral power was computed using MATLAB's wavelet method (The MathWorks), cwt (Continuous wavelet transform), with Morlet wavelets. We separately analyzed the power over three different frequency bands, namely theta (4–12 Hz), beta (13–35 Hz) and gamma (36–90 Hz) in the period of acute and chronic cisplatin administration, respectively. Theta, beta and gamma waves were filtered by bandpass filtering of LFP data. Power spectral analysis of oscillations was performed using the multi-taper method in the Matlab, setting a window length of 2 s and the time process is divided into 1 s period with 90% overlap. The power was expressed as decibels by computing 10 × log10 of the output and standardized.

The phase-amplitude coupling is used to indicate the amplitude of the high-frequency oscillation (gamma, 36–90 Hz) modulated by the average phase of the low-frequency oscillation (theta, 4–12 Hz). Modulation index (MI) is an algorithm for calculating phase-amplitude coupling, indicating the function of analytic amplitude (36–90 Hz) and analytic phase (4–12 Hz) coupling in the Arc of mice after cisplatin administration. The gamma oscillations and theta oscillations were first filtered from the LFP signal. Then the phase of theta oscillation and the amplitude of gamma oscillation was calculated from Hilbert transform.

2.7. Whole-cell recording

The *Agrp-cre*; Ai 14 mice (4-week-old) were used for whole-cell recording and deeply anesthetized with isoflurane. As described previously [26], brains were quickly removed to ice-cold oxygenated cutting solution containing (in mM): 75 sucrose, 87 NaCl, 2.5 KCl, 1.25 NaH_2PO_4, 25 $NaHCO_3$, 0.5 $CaCl_2$, 7 $MgCl_2$ and 25 glucose. Slices containing Arc region (200 μm thick) were prepared by the vibratome (VT1000S Leica) and then transferred to normal artificial cerebrospinal fluid containing (in mM): 124 NaCl, 3 KCl, 1.25 NaH_2PO_4, 26 $NaHCO_3$, 2 $CaCl_2$, 1 $MgSO_4$ and 10 glucose; for 30 min at 34 °C and maintained at 24 ± 1 °C for additional 1 h. All external solutions were saturated with 95% O_2/2.5% CO_2 gas.

Neuronal cells with tdTomato fluorescence-AgRP$^+$ neurons were visualized with a laser optics microscope equipped with a 40 × lens (Olympus). Whole-cell recording were performed in AgRP$^+$ and POMC$^+$ neurons in the Arc with a MultiClamp 700B amplifier and 1550A digitizer (Molecular Devices). Electrode resistance ranged from 4.5 to 6.5 MΩ. Neurons were held at −60 mV, with the pipette solution containing (in mM): 130 K-gluconate, 20 KCl, 10 HEPES, 0.2 EGTA, 4 Mg-ATP and 0.5 Na_3-GTP (pH was adjusted to 7.30 with KOH). Membrane properties and action potential firing were measured by current clamp recordings. The cerebral slices were incubated with SIN1 (3-Morpholinosydnonimine, Sigma, 567028, 100 μM) and UA (500 μM) for 20 min and then recorded. Data was analyzed using Clampfit 10 (Molecular Devices) and MATLAB (MathWorks). All drugs and regents were purchased from Sigma or Tocris.

2.8. Chemogenetic activation of AgRP neurons in the Arc

The *Agrp-cre* mice were anesthetized and bilaterally injected with 150 nl of *AAV-hSyn-DIO-hM3Dq-mCherry* and *AAV-hSyn-DIO-mCherry* (BrainVTA Co., Ltd, Wuhan, China) in the Arc (from bregma: anterio-posterior, −1.5 mm; medio-lateral, ±0.3 mm; dorso-ventral, −5.8 mm). *AAV-hSyn-DIO-hM3Dq-mCherry* contains the floxed inverted sequence of hM3Dq-mCherry, which is reoriented in the presence of Cre. This ensures that hM3Dq-mCherry is only expressed on AgRP neurons [27]. Cisplatin administration (6 mg/kg, i.p.) was performed after hM3Dq-mCherry expression for 21 days. After cisplatin injection for 1 h, the mice were administered with clozapine-N-oxide (CNO, C0832, Sigma, 1 mg/kg, i.p.) to activate AgRP neurons in the Arc of mice.

2.9. Bulk RNA-seq

Total RNA in the Arc of mice were extracted using RNAiso Plus (TaKaRa, Japan). We used poly-T oligomagnetic beads to purify mRNA molecules containing poly-A. Then, DNA sequencing of the libraries was performed on a BGISEQ-500 platform and data was processed by the Beijing Genomics institution (BGI, China). We screened differentially expressed genes between two groups through Expression profile by using P_value ≤ 0.05 and absolute value of Log_2 FoldChange ≥ 1. Clusterprofiler was used to perform Gene Ontology (GO) analysis ($P < 0.05$) using differentially expressed genes and pheatmap (Pretty Heatmaps, 2015) was used to display differentially expressed genes [28,29].

2.10. Cell culture

Human brain microvascular endothelial cells (HBMECs) were maintained in Dulbecco's modified Eagle's medium (DMEM, Gibco, USA) supplemented with 10% fetal bovine serum (FBS, Gibco) and 1% penicillin/streptomycin at 37 °C in 5% CO_2-humidified incubator. The HBMECs were seeded on coverslips in 24-well plates for 24 h and incubated with cisplatin (10, 50 μM) for 3 h. Then the cells were incubated with a fluorescent switch-on probe, NP3 (5 μM) at 37 °C for 30 min and performed with DAPI staining [30]. The NP3 fluorescence in cells were captured by confocal microscope.

2.11. Western blot analysis

Western blotting analysis was performed according to the method as described previously [31]. The equivalent amount of protein in lysates was separated by 10–15% SDS-PAGE and transferred to PVDF membrane (Millipore, Billerica, MA, USA). Membranes were blocked and incubated with primary antibodies as following: anti-Caspase-1 (1:1000, AdipoGen, CA, USA); anti-Nitrotyrosine (1:1000, Millipore, CA, USA); anti-β-Actin (1:5000, Sigma) at 4 °C overnight. Then, the membranes were incubated with appropriate HRP-conjugated secondary antibodies (1:5000, Life Science) for 2 h at room temperature. The proteins were visualized by an enhanced chemiluminescence detection system (Amersham Bioscience, GE Healthcare). Quantification was performed with ImageJ software (NIH, Bethesda, MA, USA).

2.12. Immunohistochemistry

Mice were anesthetized and immediately perfused with PBS and 4% paraformaldehyde (PFA) as previously described [32]. The brain was post-fixed in 4% PFA overnight and transferred to 30% sucrose in PBS. 50 μm thick sections were prepared by vibratome. Then, the brain sections were incubated with primary antibodies as following: anti-Caspase-1 (1:500, AdipoGen, CA, USA), anti-NeuN (1:300, Abcam,

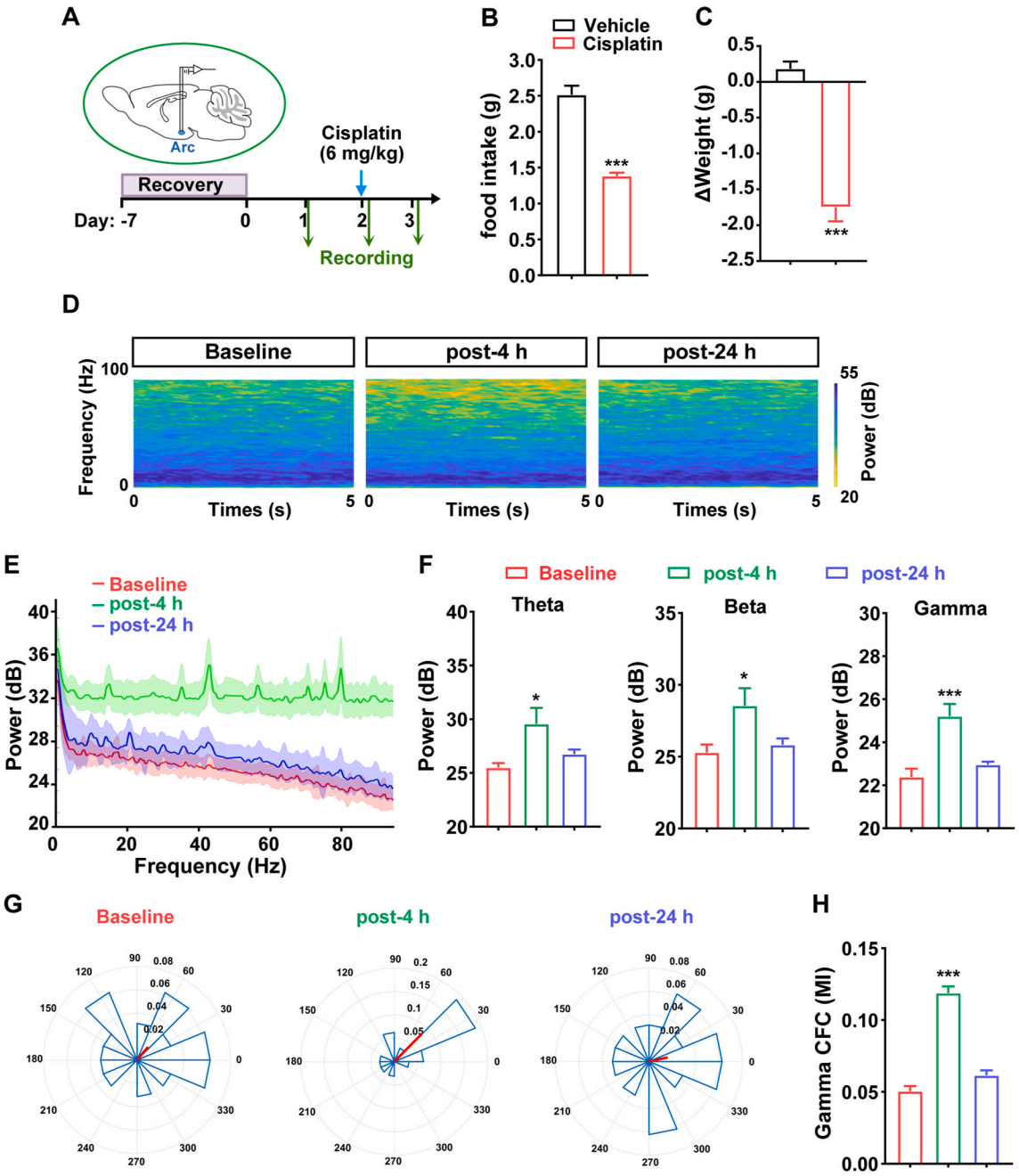

Fig. 1. Acute cisplatin administration could affect the neuronal activity in the Arc in mice. (A) Up: Schematic of electrophysiological recording in the Arc of freely moving mice. Down: The mice were intraperitoneally (i.p.) administered with 6 mg/kg cisplatin. Electrophysiological recording was carried out on 1 day before cisplatin administration, or at 4 and 24 h after cisplatin administration. (B and C) The food intake (B) and weight change (C) of mice were measured at 24 h after acute cisplatin administration. n = 6 mice. ***P < 0.001 vs Vehicle. (D) Representative spectral power (1–100 Hz) of LFP in the Arc after acute cisplatin administration. (E) LFP power (1–100 Hz) in the Arc after acute cisplatin administration (shaded areas: SEM). n = 6 mice. (F) LFP power in different frequency bands in the Arc after acute cisplatin administration. Left: power of theta oscillations (4–12 Hz); Middle: power of beta oscillations (13–35 Hz); Right: power of gamma oscillations (36–90 Hz). n = 6 mice. *P < 0.05, ***P < 0.001 vs Baseline. (G) Representative images of distribution for gamma amplitude-theta phase coupling in the Arc of mice after acute cisplatin administration. The mean vector length (red) representing coupling strength of phase with the gamma amplitude. (H) Analysis of modulation index (MI) to indicate the theta-gamma phase-amplitude coupling in the Arc of mice after acute cisplatin administration. n = 5 mice. ***P < 0.001 vs Baseline. Data were presented as mean ± SEM. (For interpretation of the references to color in this figure legend, the reader is referred to the Web version of this article.)

Cambridge, UK), anti-Lectin (1:300, DL-1177, Vector Laboratories, USA), anti-Nitrotyrosine (1:1000, Millipore, CA, USA) for overnight at 4 °C. After being rinsed three times, the sections were incubated with appropriate fluorescent secondary antibodies (Invitrogen, Carlsbad, CA) for 2 h at room temperature. Finally, the sections were stained with DAPI (0.5 μg/ml) for 5 min and mounted in Vectashield medium (Vector Laboratories, CA). Immunofluorescence images were performed with a Zeiss LSM800 confocal microscope (Carl Zeiss, Germany). The 3D surface visualization of grayscale intensity was plotted through ImageJ v1.50H and its "Interactive 3D Surface Plot" plug-in.

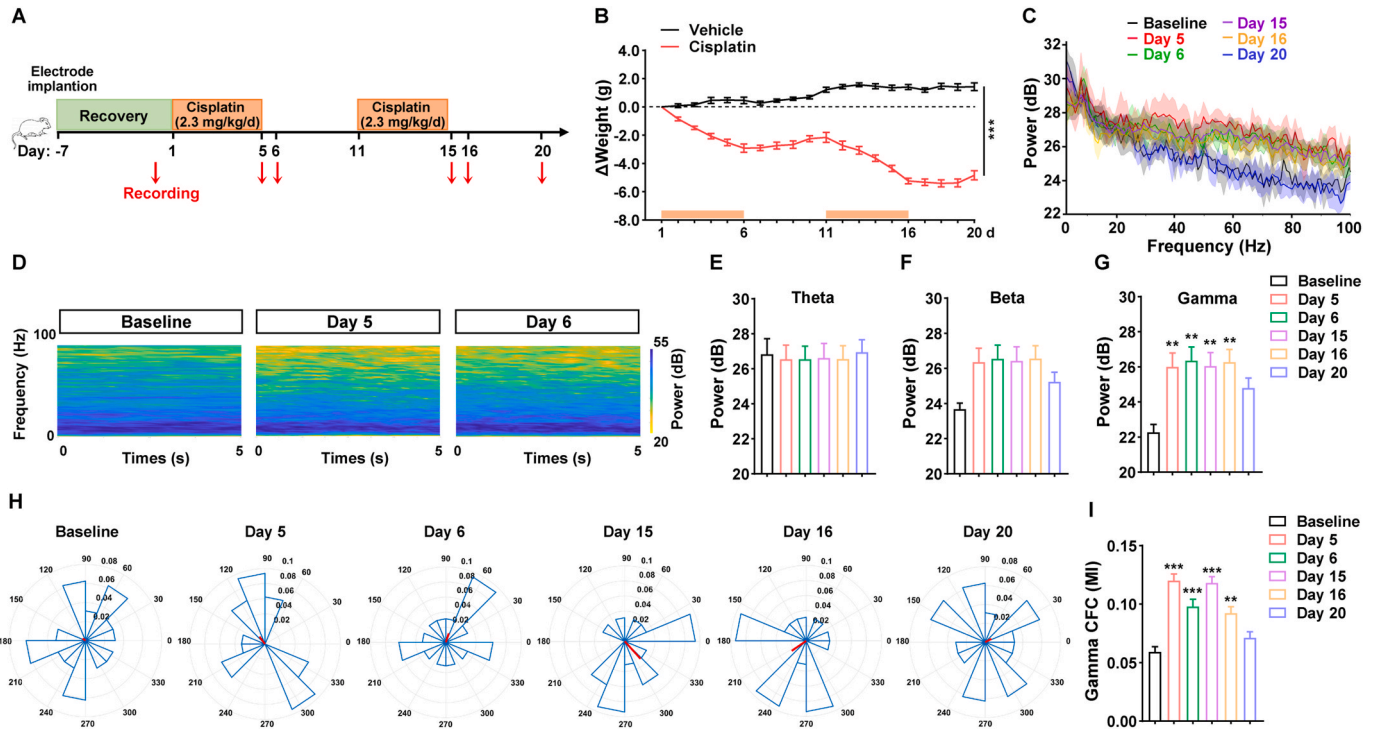

Fig. 2. Chronic cisplatin administration impaired neuronal oscillations in the Arc in mice. (A) Schematic diagram of the strategy used in mice treated with cisplatin for electrophysiological recording in the Arc for 20 days. Cisplatin was injected i.p. into mice at the dose of 2.3 mg/kg on days 1 through 5 and days 11 through 15. An electrophysiological recording was carried out on 1 day before the cisplatin administration and on the D5, D6, D15, D16 and D20 during the course of chronic cisplatin administration. (B) The weight change of mice was measured daily for 20 days with cisplatin treatment. n = 9–11 mice. ***P < 0.001 vs Vehicle on D20. (C) LFP power (1–100 Hz) in the Arc after chronic cisplatin administration (shaded areas: SEM). n = 5 mice. (D) Representative spectral power (1–100 Hz) of LFP in the Arc after chronic cisplatin administration. (E–G) LFP power in different frequency bands. Activity in the theta band (4–12 Hz) (E), in the beta band (13–35 Hz) (F) and in the gamma band (36–90 Hz) (G) in the Arc of mice after chronic cisplatin administration. n = 5 mice. **P < 0.01 vs Baseline. (H) Representative images of distribution for gamma amplitude-theta phase coupling in the Arc of mice after chronic cisplatin administration. The mean vector length (red) representing coupling strength of phase with the gamma amplitude. (I) Analysis of MI to indicate the theta-gamma phase-amplitude coupling in the Arc of mice after chronic cisplatin administration. n = 5 mice. **P < 0.01, ***P < 0.001 vs Baseline. Data were presented as mean ± SEM. (For interpretation of the references to color in this figure legend, the reader is referred to the Web version of this article.)

2.13. Statistical analysis

All data are presented as mean ± SEM. Statistical analyses were performed using GraphPad Prism 8 (GraphPad Software). Significant differences were determined by either unpaired two-tailed Student's t-test or one-way analysis of variance (ANOVA) or two-way ANOVA followed by a post-hoc Tukey's Test. Differences were considered statistically significant at $P < 0.05$.

3. Results

3.1. The effect of acute cisplatin administration on neuronal activity in the Arc of mice

Neurotoxicity caused by cisplatin is a major obstacle during chemotherapy [5]. Here, we first examined the effects of cisplatin on food consumption and the weight of mice. The food intake and weight of mice were significantly decreased 24 h after cisplatin administration (Fig. 1A–C). It is noteworthy that the Arc in the hypothalamus plays a central role in control of feeding behavior; thus, there is increasing the interesting to investigate whether the feeding behavior disorder in the context of cisplatin exposure is related to the Arc. Thus, we further measured neuronal activity in the Arc of mice during spontaneous behavior after acute cisplatin administration by *in vivo* electrophysiological recording (Fig. 1A). The power of theta (4–12 Hz), beta (13–35 Hz), and gamma (36–90 Hz) oscillations significantly increased in the Arc of mice after cisplatin treatment for 4 h (Baseline, recorded 24 h before cisplatin administration) (Fig. 1D–F). Oscillations in these frequency bands may occur simultaneously and can interact with each other [33]. It has been suggested that cross-frequency coupling (CFC) plays a vital role in neuronal signal processing [34]. Importantly, the high-frequency amplitude can be modulated by the phase of slow brain rhythms simultaneously, such as theta-to-gamma phase-amplitude coupling [34]. Interestingly, standard phase-amplitude coupling analysis of LFPs demonstrated that the theta-gamma phase-amplitude coupling increased significantly in the Arc of the mice after cisplatin administration for 4 h (Fig. 1G and H, Supplemental Fig. 1A). Together, these findings indicated that after acute cisplatin administration, mice have impaired neuronal oscillations and theta-gamma phase-amplitude coupling dysfunction in the Arc.

3.2. Chronic cisplatin administration impaired neuronal oscillations in the Arc of mice

We mimicked the clinical cisplatin treatment regimen for patients with cancer to further confirm the effects of cisplatin on neuronal activity in the Arc in mice. The mice were administered with 2.3 mg/kg cisplatin for 5 days, and followed by 5 days of rest for a total of 20 days (Fig. 2A). As shown in Fig. 2B, the cisplatin-injected mice displayed a significant weight decrease compared with vehicle-treated mice from Day 2 (D2). Similarly, we also investigated neuronal activity in the Arc of mice after chronic cisplatin administration. Compared to those of vehicle-treated mice, the gamma oscillations (30–90 Hz) increased significantly on D5, D6, D15, and D16 in the Arc of cisplatin-treated

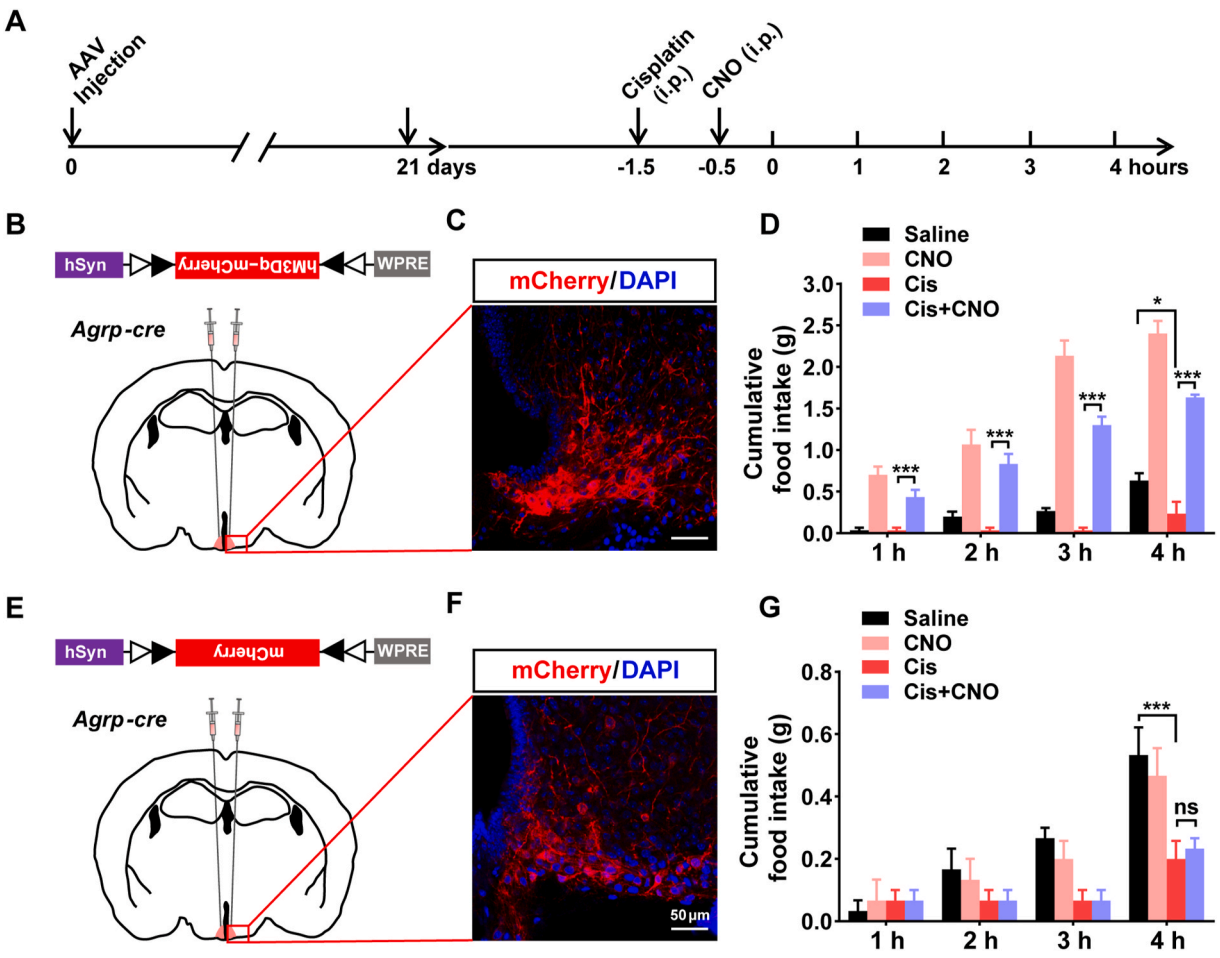

Fig. 3. Chemogenetic activation of AgRP neurons reversed the cisplatin-induced decrease in food intake of mice. (A) Experimental protocol for activation of the AgRP neuron induced by clozapine-N-oxide (CNO) and cisplatin treatment in mice. Cisplatin administration (6 mg/kg, i.p.) was performed after hM3Dq-mCherry expression for 21 days. After cisplatin injection for 1 h, the mice were administered with CNO (1 mg/kg, i.p.) to activate AgRP neurons. (B and E) *AAV-hSyn-DIO-hM3Dq-mCherry* (B) and *AAV-hSyn-DIO-mCherry* (E) were injected into the Arc of hypothalamus in *Agrp-cre* mice. (C and F) Representative immunofluorescence staining of mCherry (red) and DAPI (blue) in the Arc of *Agrp-cre* mice. Scale bar = 50 μm. (D and G) The cumulative food intake of mice treated with cisplatin and CNO. n = 3 mice. *P < 0.05, ***P < 0.001. ns: No significant difference. Data were presented as mean ± SEM. (For interpretation of the references to color in this figure legend, the reader is referred to the Web version of this article.)

mice, whereas no such dynamics were observed for the theta and beta oscillations of mice (Fig. 2C–G). In addition, standard phase-amplitude coupling analysis of LFPs showed an obvious increase in theta-gamma phase-amplitude coupling on D5, D6, D15, and D16 in the Arc of mice after chronic administration of cisplatin (Fig. 2H and I, Supplemental Fig. 1B). Taken together, these observations suggested that chronic cisplatin administration could induce impaired gamma oscillations and theta-gamma phase-amplitude coupling dysfunction in the Arc of mice, which might be related to the feeding behavior disorder mediated by cisplatin.

3.3. Chemogenetic activation of AgRP neurons reversed the cisplatin-induced decrease in food intake in mice

AgRP and POMC neurons in the Arc play a key role in regulating food intake and body weight [35]. Given the essential role of AgRP neurons, which release AgRP and NPY and promote feeding [36,37], we sought to investigate whether AgRP neurons in the Arc contribute to the feeding behavior disorder induced by cisplatin (Fig. 3A). We performed *Agrp-cre* mice with *AAV-hSyn-DIO-hM3Dq-mCherry* (Fig. 3B) and *AAV-hSyn--DIO-mCherry* (Fig. 3E) through the combined use of Cre-dependent adeno-associated viruses (AAVs) with restricted designer receptors exclusively activated by designer drugs (DREADDs) in AgRP neurons and CNO to pharmacogenetically activate AgRP neurons *in vivo*. 21 days after virus injection, the mice were treated with cisplatin and CNO and their food intake was evaluated for another 4 consecutive hours (Fig. 3A). Confocal images showed that mCherry fluorescence was efficiently expressed in a Cre-dependent manner in the Arc of *Agrp-cre* mice (Fig. 3C and F). Interestingly, the activation of AgRP neurons by CNO reversed the cisplatin-induced decrease in food intake in mice (Fig. 3D). The control virus had no obvious effects on the food intake of cisplatin-treated mice (Fig. 3G). All these results indicated that selective activation of AgRP neurons could reverse the cisplatin-induced abnormal food intake in mice.

3.4. Cisplatin activated caspase-1 in the Arc of mice

To elucidate the molecular mechanisms underlying neuronal oscillation dysfunction mediated by cisplatin, we performed the RNA sequencing analysis of cells sorting from the Arc of mice after treatment with cisplatin or vehicle. We screened for differentially expressed genes by using a P_value ≤ 0.05 and $|\log_2 \text{FoldChange}| \geq 1$. Then, we evaluated 973 differentially expressed genes using GO analysis, which revealed an alteration in pathways related to cisplatin-induced feeding behavior disorder. We focused on the regulation of inflammatory response pathway, which is important in control of Arc neuronal activity and

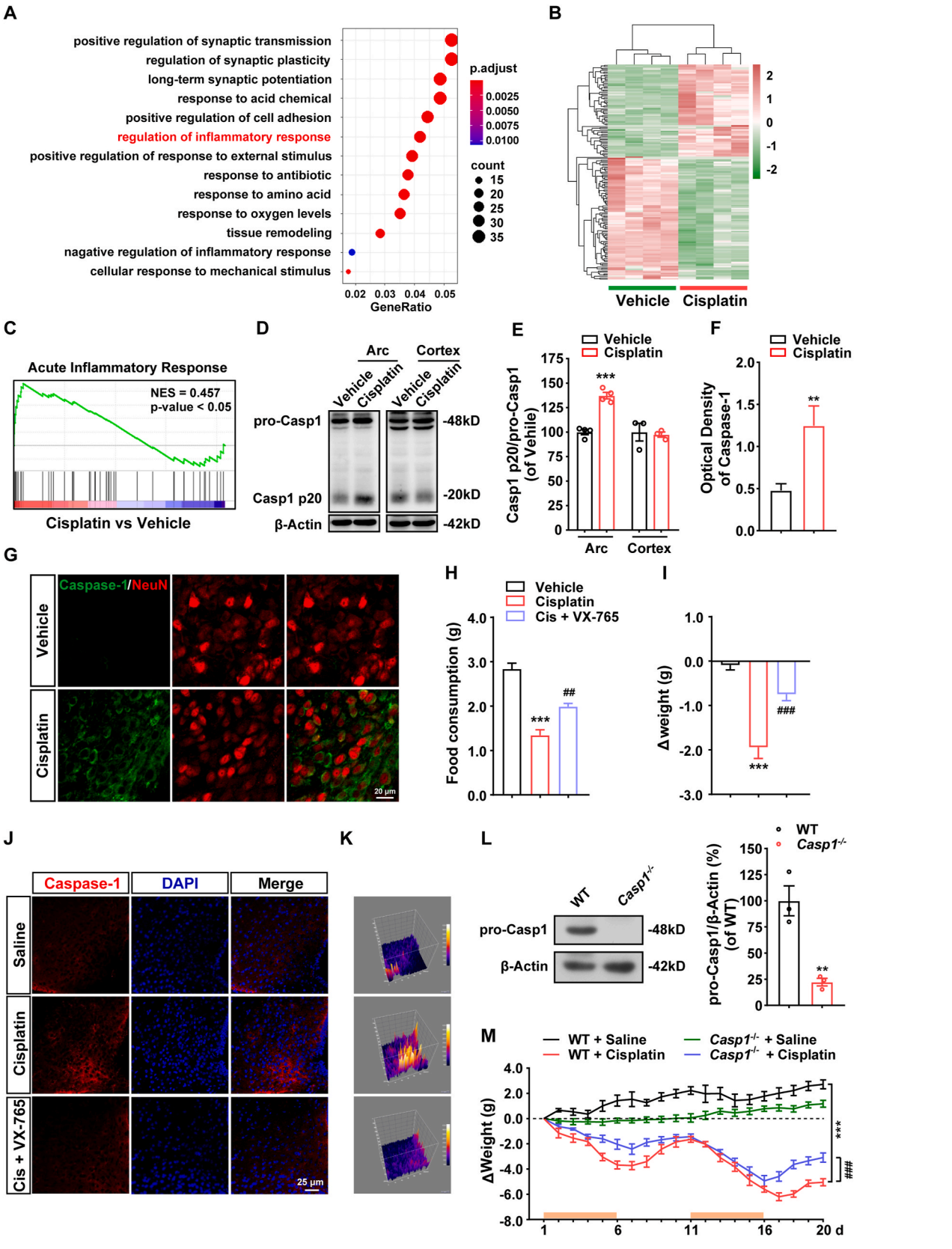

(caption on next page)

Fig. 4. Cisplatin activated caspase-1 in the Arc in mice. (A) GO analysis of pathways enriched for the 973 genes that are more differentially expressed in cisplatin-treated mice. (B) Heat map of normalized expression for 159 selected genes ($P \leq 0.05$ & $|\log_2 FC| \geq 1$) between vehicle-treated and cisplatin-treated mice. The color scale of the heat map indicated fold changes of expression for each gene: red, upregulation. (C) Gene Set Enrichment Analysis (GSEA) showed the acute inflammatory response signaling pathway was highly expressed in the Arc of mice treated with cisplatin. (D and E) Representative Western blot of caspase-1 and β-Actin in the Arc and cortex of mice after chronic cisplatin administration for 20 days (D) and quantitative analysis (E). n = 3 mice. ***P < 0.001 vs Vehicle. (F and G) Representative immunofluorescence staining of Caspase-1 (green) and NeuN (red) in the Arc of mice treated with cisplatin (G) and quantitative analysis (F). n = 8 mice. **P < 0.01 vs Vehicle. Scale bar = 20 μm. (H and I) The food intake (H) and weight change (I) of mice were measured 24 h after cisplatin administration combined with VX-765. n = 9–13 mice. ***P < 0.001 vs Vehicle; ##P < 0.01, ###P < 0.001 vs Cisplatin. (J) Representative immunofluorescence staining of Caspase-1 (red) and DAPI (blue) in the Arc of mice administered with cisplatin combined with VX-765. Scale bar = 25 μm. (K) The 3D surface visualization of intensity of Caspase-1 and DAPI signals from (J). (L) Western blotting assay of caspase-1 and β-Actin in the Arc of *Casp1*$^{-/-}$ mice (Left) and quantitative analysis (Right). **P < 0.01 vs WT. (M) The weight change of WT and *Casp1*$^{-/-}$ mice treated with cisplatin or vehicle was measured daily for total 20 days. n = 4–8 mice. ***P < 0.001: WT + Saline vs WT + Cisplatin; ###P < 0.001: WT + Cisplatin vs *Casp1*$^{-/-}$ + Cisplatin on D20. Data were presented as mean ± SEM. (For interpretation of the references to color in this figure legend, the reader is referred to the Web version of this article.)

feeding behavior (Fig. 4A). The comparison of the heat map for 159 inflammation-related genes between the vehicle-treated group and cisplatin-treated group revealed a clearly different signature (Fig. 4B). In addition, the acute inflammatory response signaling pathway was highly expressed in the Arc of cisplatin-treated mice, as determined through Gene Set Enrichment Analysis (GSEA) (Fig. 4C) [29].

Considering the inflammatory response after cisplatin treatment, we measured the canonical effector protein downstream of the most fully characterized inflammasomes, caspase-1, which can process interleukin-1 family members [38]. Interestingly, the results showed that Casp1 p20 levels were elevated in the Arc of mice but not in the cortex after cisplatin treatment (Fig. 4D and E). Furthermore, subsequent immunofluorescence staining showed that caspase-1 was highly expressed in the Arc neurons of cisplatin-treated mice (Fig. 4F and G). In addition, lipopolysaccharide (LPS) administration into the Arc of mice attenuated the food intake and weight of mice, indicating the crucial role of elevated inflammation (particularly caspase-1) in the Arc in the feeding behavior of mice (Supplemental Fig. 2). All these results suggested that cisplatin could activate caspase-1 in the Arc in mice, which might be related to abnormal feeding behavior.

3.5. Caspase-1 deficiency alleviated the abnormal feeding behavior induced by cisplatin in mice

To further explore the potential role of caspase-1 in the abnormal feeding behavior induced by cisplatin, the mice were treated with the caspase-1 inhibitor VX-765. Caspase-1 inhibition with VX-765 increased food intake and inhibited the weight loss induced by cisplatin (Fig. 4H and I). Moreover, the caspase-1 level in the Arc was significantly attenuated by VX-765 pretreatment (Fig. 4J and K). Furthermore, caspase-1-deficient (*Casp1*$^{-/-}$) mice were used to investigate the role of caspase-1 in cisplatin treatment (Fig. 4L). Cisplatin-induced weight loss was markedly attenuated in *Casp1*$^{-/-}$ mice compared to WT mice (Fig. 4M). Taken together, these evidences indicated that cisplatin activated caspase-1 in the Arc of mice, and caspase-1 deficiency could alleviate the abnormal feeding behavior induced by cisplatin.

3.6. $ONOO^-$ formation in the Arc was involved in cisplatin-mediated neurotoxicity

To clarify the mechanism of cisplatin-mediated caspase-1 activation in Arc neurons, we first examined the concentration of cisplatin in the Arc and found that cisplatin was undetectable in the Arc of mice both 4 h and 20 days after cisplatin treatment (Supplemental Fig. 3). Based on our previous study, brain endothelial $ONOO^-$ is a reactive product generated from the reaction of nitric oxide ($NO^•$) with superoxide ($O_2^{•-}$) under pathological contexts, which could trigger neuronal dysfunction and cell death [30,39]. Therefore, we analyzed the $ONOO^-$ levels of endothelial cells exposed to cisplatin. The NP3 probe was used to detect the living intracellular $ONOO^-$ generation after HBMECs were incubated with cisplatin for 3 h. The intracellular fluorescence gradually increased in a dose-dependent manner after cisplatin stimulation (Fig. 5A). Moreover, compared to vehicle treatment, cisplatin treatment significantly increased the levels of nitrotyrosine in the Arc of mice, mainly in endothelial cells (Fig. 5B–E). Interestingly, UA, a known natural scavenger of $ONOO^-$, attenuated the elevated levels of nitrotyrosine and caspase-1 induced by cisplatin in the Arc of mice, which implied the important role of $ONOO^-$ in cisplatin-mediated caspase-1 activation (Fig. 5D–F). These evidences indirectly indicated that the overproduction of $ONOO^-$ in the Arc was involved in cisplatin-mediated neurotoxicity.

3.7. Endothelial $ONOO^-$ affected the excitability of AgRP and POMC neurons in the Arc

To specifically characterize the effects of $ONOO^-$ on AgRP and POMC neurons in the Arc, we used *ex vivo* electrophysiology to record the resting membrane potential (RMP) and action potential of the AgRP and POMC neurons in acute separated cerebral slices. We first obtained *Agrp-cre;* Ai14 mice by crossing *Agrp-Cre* mice with Ai14 mice, which expressed tdTomato fluorescence following Cre-dependent recombination [40]. As shown in Fig. 5G, tdTomato fluorescence was efficiently expressed in the Arc. We distinguished AgRP-positive neurons and POMC-positive neurons by observing whether they expressed red fluorescence and performed whole-cell recording (Supplemental Fig. 4A). After treatment with SIN1, as an $ONOO^-$ donor, AgRP neurons emitted significantly fewer AP spikes than the control group. In contrast, pre-incubation with UA could reversed the reduced AP frequency caused by SIN1, suggesting the salvaging effect of UA on SIN1-induced neuronal injuries (Fig. 5H and I). In addition, SIN1 decreased the amplitude and increased the half-width of the AP in AgRP neurons (Fig. 5J and L) without changing the release threshold or afterhyperpolarization (AHP) current (Fig. 5K and M). Strikingly, SIN1-induced impairments in AP properties were alleviated by UA treatment (Fig. 5J and L). There was no difference in the RMP of AgRP neurons treated with SIN1 and/or UA (Fig. 5N). Similarly, we also recorded the effects of SIN1 and UA on POMC neurons. In contrast to AgRP neurons, the AP frequency of POMC neurons increased significantly under SIN1 treatment and was attenuated by UA pretreatment (Supplemental Fig. 4B), whereas other AP properties (amplitude, AHP, AP firing threshold and RMP) did not change (Supplemental Fig. 4C-G). According to *ex vivo* electrophysiological results, we further evaluated the cerebral slices by Western blotting analysis to explore the important role of $ONOO^-$ in caspase-1 activation mediated by cisplatin in the Arc. Strikingly, SIN1 significantly increased the expression of Casp1 p20 in the Arc of the cerebral slices, and this SIN1-induced increase in Casp1 p20 expression could be inhibited by UA treatment (Fig. 5O and P).

In summary, these results indicated that endothelial $ONOO^-$ generation by cisplatin decreased the excitability of AgRP neurons and lead to POMC neuron hyperacitivity, while UA provided a protective effect against the insults induced by $ONOO^-$.

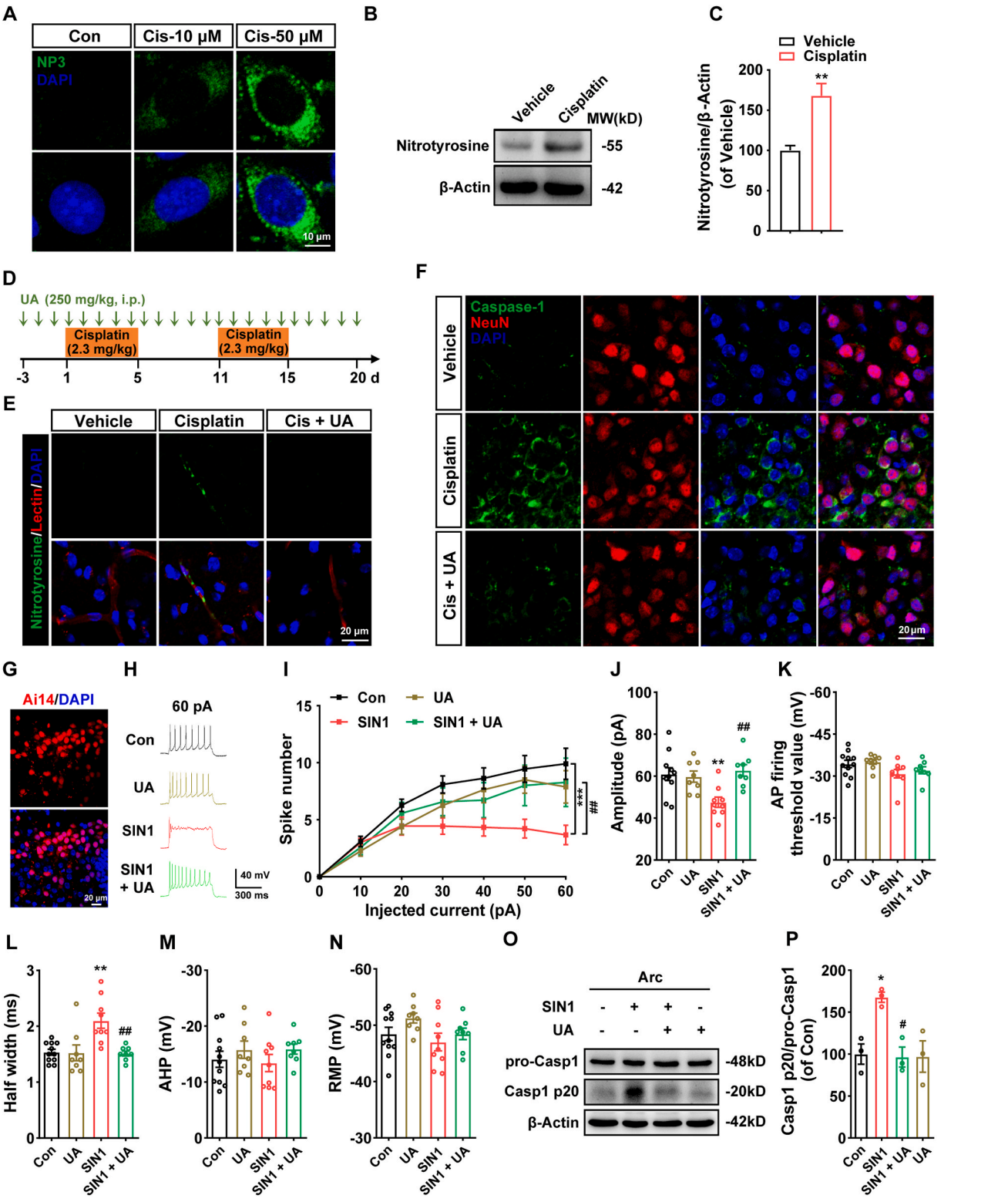

(caption on next page)

Fig. 5. Endothelial ONOO$^-$ in the Arc was involved in cisplatin-mediated neurotoxicity by targeting caspase-1. (A) Representative confocal images showed the ONOO$^-$ level (green) and DAPI (blue) in HBMECs after cisplatin treatment. HBMECs were exposed to cisplatin (10, 50 μM) for 3 h and the ONOO$^-$ level was detected by the NP3 probe in living cells. Scale bar = 10 μm. (B and C) Representative Western blot of Nitrotyrosine and β-Actin in the Arc of mice after chronic cisplatin administration for 20 days (B) and quantitative analysis (C). n = 4 mice. **P < 0.01 vs Vehicle. (D) Experimental protocol used to treat mice with UA and cisplatin. UA (i.p.) was pretreated at the dose of 250 mg/kg before cisplatin administration for 3 days. UA was administered daily before cisplatin injection for 6 h and continuously for another 20 days. (E) Representative immunofluorescence staining of Nitrotyrosine (green), Lectin (red, a marker for blood vessels) and DAPI (blue) in the Arc of mice treated with cisplatin or UA. Scale bar = 20 μm. (F) Representative immunofluorescence staining of Caspase-1 (green), NeuN (red) and DAPI (blue) in the Arc of mice treated with cisplatin or UA. Scale bar = 20 μm. (G) Representative immunofluorescence staining of Ai14 (red) and DAPI (blue) in the Arc of *Agrp-cre*; Ai 14 mice. Scale bar = 20 μm. (H) Representative AP firing traces in the AgRP-positive neurons evoked by current injections (60 pA). (I) Number of AP firing in AgRP neurons evoked by current injections from 0 to 60 pA in the Arc of cerebral slices. ***P < 0.001: Con vs SIN1; ##P < 0.01: SIN1 vs SIN1 + UA on 60 pA. (J–M) Whole-cell patch clamps were used to detect AP properties of AgRP neurons, including AP amplitude (J), AP firing threshold (K), AP half-width (L) and AHP (M). (N) UA and SIN1 had no effects on RMP of AgRP neurons. Con: n = 11 cells from 6 mice; UA: n = 8 cells from 3 mice; SIN1: n = 9 cells from 4 mice; SIN1 + UA: n = 8 cells from 3 mice. **P < 0.01 vs Con; ##P < 0.01 vs SIN1. (O and P) Representative Western blot of caspase-1 and β-Actin in the Arc of cerebral slices after *ex vivo* electrophysiological analysis (O) and quantitative analysis (P). Above experiments were repeated three times independently. *P < 0.05 vs Con; #P < 0.05 vs SIN1. Data were presented as mean ± SEM. (For interpretation of the references to color in this figure legend, the reader is referred to the Web version of this article.)

3.8. The ONOO$^-$ scavenger UA normalized the abnormal neuronal oscillations in the Arc in cisplatin-induced neurotoxicity

To further prove that ONOO$^-$ in the Arc affected the excitability of AgRP and POMC neurons, we examined neuronal oscillations in the Arc of mice after treatment with cisplatin and UA. First, we found that the clearance of ONOO$^-$ with UA could attenuate the weight loss of mice induced by cisplatin (Fig. 6A). Second, *in vivo* electrophysiological recordings in the Arc of mice showed significant increased gamma band activity (30–90 Hz) on D5, D6, D15, and D16 after cisplatin administration, and this increased gamma band activity could be inhibited by UA treatment on D15 and D16 (Fig. 6B–D and G). However, no such dynamics were revealed in the theta and beta band activity of mice treated with cisplatin, UA, cisplatin + UA or not on D15 (Fig. 6C–F). Finally, an increase in theta-gamma phase-amplitude coupling on D15 after chronic cisplatin treatment could be alleviated by UA administration (Fig. 6H and I). Taken together, these observations suggested that targeting endothelial peroxynitrite could normalize abnormal neuronal gamma oscillations and neuronal theta-gamma phase-amplitude coupling in the Arc impaired by cisplatin.

4. Discussion

Severe toxicity caused by high-dose cisplatin therapy limits its application [5]. However, there are no effective treatments or preventive measures available for the anorexia, weight loss and neurotoxicity associated with cisplatin treatment. The present study demonstrated that cisplatin treatment could affect neuronal gamma oscillations, induce local theta-gamma phase-amplitude coupling dysfunction, and mediate feeding behavior disorder. Remarkably, our findings further showed that endothelium-derived ONOO$^-$ induced AP firing dysfunction and caspase-1 activation in the Arc neurons under cisplatin treatment, which were ameliorated by the ONOO$^-$ scavenger UA (Fig. 6J). Endothelial ONOO$^-$ mediating cisplatin-induced neurotoxicity through neuronal caspase-1 activation provides a new working model for cisplatin-induced feeding behavior disorder, which can shed light on new drug targets and candidate drugs for the prevention of the neurotoxicity, anorexia and weight loss induced by cisplatin.

To the best of our knowledge, this is the first study to report that Arc neuronal oscillations, especially gamma oscillations, participate in feeding behavior under cisplatin treatment. Gamma-rhythmic input to the lateral hypothalamus has been shown to evoke food approaches without affecting food intake [41]. Here, we first found, under 32-channel electrode recording in the Arc of free-moving mice, an increase in the power of theta (4–12 Hz), beta (13–35 Hz) and gamma (36–90 Hz) oscillations in the neurons of the Arc under acute cisplatin treatment, and chronic cisplatin treatment significantly enhanced gamma band activity. Notably, neuronal gamma oscillations in the Arc of mice were associated with feeding behavior under cisplatin exposure. In brain networks, cross-frequency phase-amplitude coupling has been well documented and can occur independently between two rhythms. On the other hand, the two oscillations could emerge from the same neuronal substrate [42,43]. Surprisingly, no compelling evidence has been shown for a functional role for the best-known theta-gamma phase-amplitude coupling observed in the Arc. Specifically, our data from the phase-amplitude coupling analysis indicated clear modulation of gamma (36–90 Hz) amplitudes by the theta phase under both in acute and chronic cisplatin administration. Neuronal oscillations are a natural mechanism for forming cell assemblies, and are mostly reported in the cerebral cortex and hippocampus [44]. Our studies have widely expanded the neuronal gamma oscillations and theta-gamma phase-amplitude coupling in the Arc under cisplatin treatment.

The underlying molecular complexity of feeding behavior disorder and how it relates to cisplatin-induced abnormal neuronal oscillations are only beginning to be unraveled. Previous work has shown that NLRP3 inflammasome-caspase-1 signaling not only underlies antitumor effects of cisplatin in triple-negative breast cancer [45], but also triggers ototoxicity and nephrotoxicity [18,19,46]. Here, our findings clarified that caspase-1 activation in Arc neurons was one of the key biochemical signals involved in cisplatin-induced feeding behavior disorder. Caspase-1 inhibitor or caspase-1 knockout improved the food intake and ameliorated weight loss after cisplatin treatment. It is well established that two key populations of cells within the Arc of hypothalamus, AgRP and POMC neurons, exert opposing actions on food intake [47–49]. Herein, chemogenetic activation of AgRP neurons in the Arc reversed the cisplatin-induced decrease in food intake.

ONOO$^-$ is generated upon the reaction of $O_2^{\bullet-}$ and $NO^{\bullet}$ and can chemically modify proteins, subsequently modulating downstream signaling [50]. The high concentration of $O_2^{\bullet-}$ induced by uncoupled eNOS can quickly react with iNOS-induced $NO^{\bullet}$, resulting in abnormal ONOO$^-$ formation [51,52]. ONOO$^-$ has been reported to be associated with various redox-related diseases [24,53]. To explore whether ONOO$^-$ was involved in cisplatin-induced damage, we used NP3 (an ONOO$^-$ probe) to monitor ONOO$^-$ generation in living HBMECs. We found that intracellular ONOO$^-$ generation increased significantly in the HBMECs and endothelial cells of cerebral microvessels after cisplatin exposure.

Interestingly, endothelium-derived ONOO$^-$ induced by cisplatin initiated caspase-1 activation in the Arc neurons of mice. Our results showed that UA eliminated caspase-1 activation in the Arc neurons induced by cisplatin. Similarly, under whole-cell patch current clamp recording, SIN1, as an ONOO$^-$ donor, decreased the AP frequency in AgRP neurons and increased the AP frequency in POMC neurons in the Arc, which were abolished by UA treatment. More importantly, UA normalized the abnormal neuronal gamma oscillations and neuronal theta-gamma phase-amplitude coupling in the Arc involved in cisplatin-induced feeding behavior disorder. Thus, the findings of the present study suggest the potential role of endothelium-derived ONOO$^-$ and caspase-1 in Arc neurons in cisplatin-induced neurotoxicity and feeding behavior disorder. Investigating the effect of UA on cisplatin anorexia in

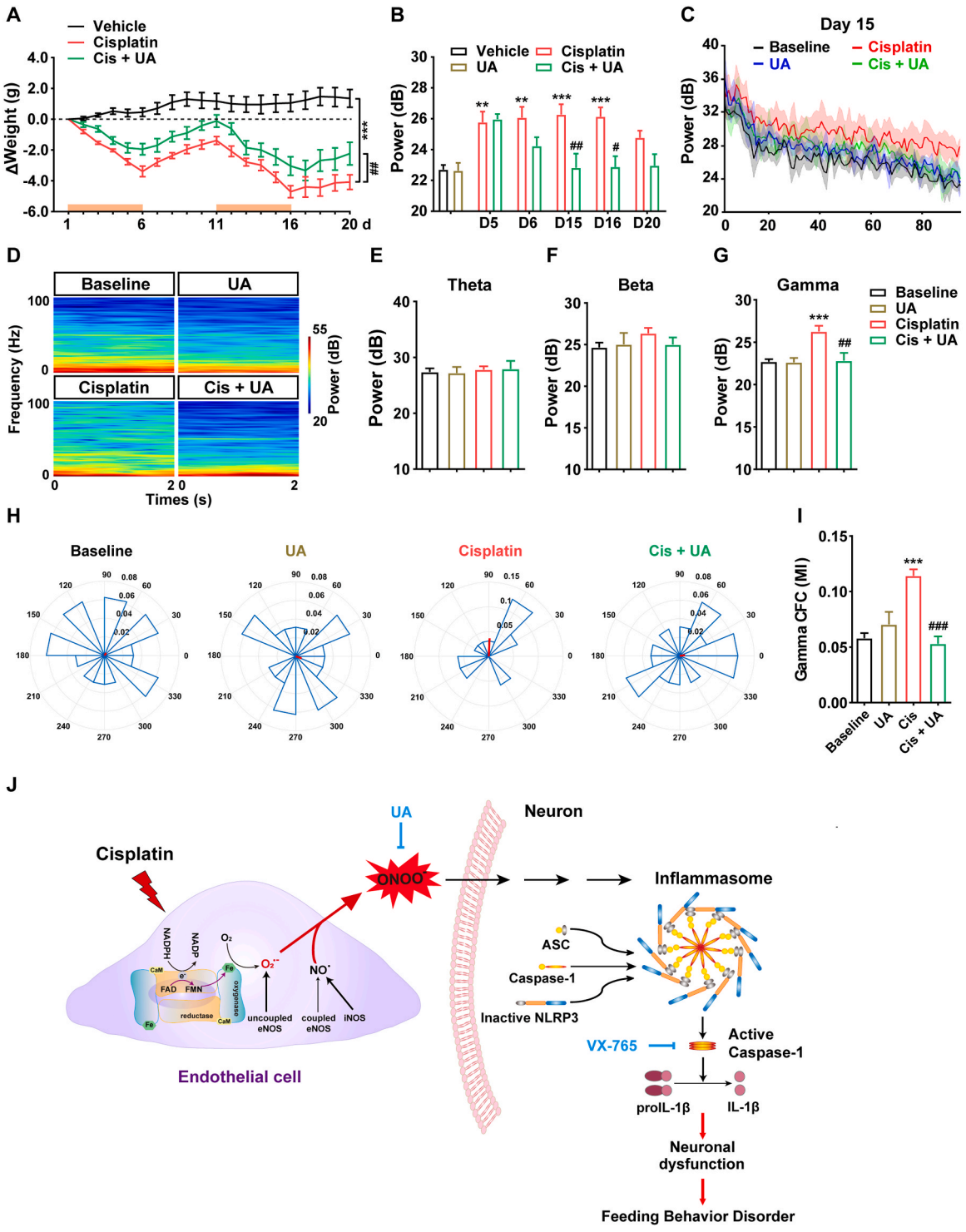

Fig. 6. The ONOO⁻ scavenger normalized abnormal neuronal oscillations in cisplatin-induced neurotoxicity in the Arc. (A) The weight change of mice were measured daily for a total of 20 days. n = 6 mice. ***P < 0.001: Vehicle vs Cisplatin; ##P < 0.01: Cisplatin vs Cis + UA on D20. (B) LFP power of gamma oscillations (36–90 Hz) in the Arc of mice after chronic cisplatin administration. n = 5–11 mice. **P < 0.01, ***P < 0.001 vs Vehicle; ##P < 0.01, #P < 0.05: Cisplatin vs Cis + UA on D15 and D16, respectively. (C) LFP power (1–100 Hz) in the Arc of mice on D15 after chronic cisplatin administration (shaded areas: SEM). n = 5–6 mice. (D) Representative spectra (1–100 Hz) of LFP in the Arc of mice on D15 after chronic cisplatin administration. (E–G) LFP power in different frequency bands. Activity in the theta band (4–12 Hz) (E), in the beta band (13–35 Hz) (F) and in the gamma band (36–90 Hz) (G) in the Arc of mice on D15 after chronic cisplatin administration. n = 5–6 mice. ***P < 0.001 vs Baseline; ##P < 0.01 vs Cisplatin. (H) Representative images of distribution for gamma amplitude-theta phase coupling in the Arc of mice on D15 after chronic cisplatin administration. The mean vector length (red) representing coupling strength of phase with the gamma amplitude. (I) Analysis of MI to indicate the theta-gamma phase-amplitude coupling in the Arc of mice on D15 after chronic cisplatin administration. n = 5–11 mice. ***P < 0.001 vs Baseline; ###P < 0.001 vs Cisplatin. (J) A scheme for the proposed mechanisms underlying the cisplatin-induced feeding behavior disorder. Data were presented as mean ± SEM. (For interpretation of the references to color in this figure legend, the reader is referred to the Web version of this article.)

the context of cancer in future studies may help optimize UA efficacy and avoid side effects. Although the new complexes of platinum (Pt) generated through modifications of Pt-based molecules showed lower cross-resistance of tumor cells and higher antitumor effects [54], their potential neurotoxic effect is still worthy of attention during clinical practice.

Taken together, our novel data presented here demonstrated that the communication of endothelium-derived $ONOO^-$ and neuronal caspase-1 activation was involved in abnormal neuronal gamma oscillations in the Arc and mediated neurotoxicity under cisplatin treatment. Strengthening the protection of the vascular endothelium and regulating caspase-1 signaling may alleviate cisplatin-induced anorexia and weight loss.

Author contributions

ML.S. designed research studies, conducted experiments, acquired and analyzed data and wrote the manuscript. XF.M. performed the *in vivo* electrophysiology and L.L. performed the ex vivo electrophysiology. ZM.L., ZH.Z. and DM.G. assisted with methodology. X.C. assisted with bioinformatics analysis. Y.Z., K.F. and Y.J. reviewed and edited paper. AH.G., YM.L. and F.H. conceived the study, secured funding, supervised the work, writing-review and editing.

Declaration of competing interest

The authors have declared that no conflict of interest exists.

Acknowledgements

This work was supported by the State Key Program of National Natural Science Foundations of China (81730101 and 81930103 to F. H.); National Natural Science Foundations of China (81973300 to YM.L.; 82003731 to ML.S.); Chinese Postdoctoral Science Foundations (2020M671549 to ML.S.).

Appendix A. Supplementary data

Supplementary data related to this article can be found at https://doi.org/10.1016/j.redox.2021.102147.

References

[1] L. Kelland, The resurgence of platinum-based cancer chemotherapy, Nat. Rev. Canc. 7 (8) (2007) 573–584.
[2] L. Grassi, et al., Role of psychosocial variables on chemotherapy-induced nausea and vomiting and health-related quality of life among cancer patients: a European study, Psychother. Psychosom. 84 (6) (2015) 339–347.
[3] J.T. Hickok, et al., Nausea and emesis remain significant problems of chemotherapy despite prophylaxis with 5-hydroxytryptamine-3 antiemetics: a University of Rochester James P. Wilmot Cancer Center Community Clinical Oncology Program Study of 360 cancer patients treated in the community, Cancer 97 (11) (2003) 2880–2886.
[4] P.J. Hesketh, et al., Antiemetics: American society of clinical oncology clinical practice guideline update, J. Clin. Oncol. 35 (28) (2017) 3240–3261.
[5] S.B. Park, et al., Chemotherapy-induced peripheral neurotoxicity: a critical analysis, CA Cancer J. Clin. 63 (6) (2013) 419–437.
[6] M.J. McKeage, et al., Nucleolar damage correlates with neurotoxicity induced by different platinum drugs, Br. J. Canc. 85 (8) (2001) 1219–1225.
[7] M.G. Myers Jr., D.P. Olson, Central nervous system control of metabolism, Nature 491 (7424) (2012) 357–363.
[8] J.H. Jeong, D.K. Lee, Y.H. Jo, Cholinergic neurons in the dorsomedial hypothalamus regulate food intake, Mol. Metab. 6 (3) (2017) 306–312.
[9] G.D. Stuber, R.A. Wise, Lateral hypothalamic circuits for feeding and reward, Nat. Neurosci. 19 (2) (2016) 198–205.
[10] E. Yulyaningsih, et al., Acute lesioning and rapid repair of hypothalamic neurons outside the blood-brain barrier, Cell Rep. 19 (11) (2017) 2257–2271.
[11] S. Morita-Takemura, A. Wanaka, Blood-to-brain communication in the hypothalamus for energy intake regulation, Neurochem. Int. 128 (2019) 135–142.
[12] Q. Wei, et al., Uneven balance of power between hypothalamic peptidergic neurons in the control of feeding, Proc. Natl. Acad. Sci. U. S. A. 115 (40) (2018) E9489–E9498.
[13] E. Gropp, et al., Agouti-related peptide-expressing neurons are mandatory for feeding, Nat. Neurosci. 8 (10) (2005) 1289–1291.
[14] S.M. Sternson, G.M. Shepherd, J.M. Friedman, Topographic mapping of VMH–> arcuate nucleus microcircuits and their reorganization by fasting, Nat. Neurosci. 8 (10) (2005) 1356–1363.
[15] B.H. Ali, et al., Effect of concomitant treatment of curcumin and melatonin on cisplatin-induced nephrotoxicity in rats, Biomed. Pharmacother. 131 (2020) 110761.
[16] Y. Dai, et al., Calcitriol inhibits ROS-NLRP3-IL-1beta signaling axis via activation of Nrf2-antioxidant signaling in hyperosmotic stress stimulated human corneal epithelial cells, Redox Biol. 21 (2019) 101093.
[17] J.M. Abais, et al., Redox regulation of NLRP3 inflammasomes: ROS as trigger or effector? Antioxidants Redox Signal. 22 (13) (2015) 1111–1129.
[18] S. Faubel, et al., Caspase-1-deficient mice are protected against cisplatin-induced apoptosis and acute tubular necrosis, Kidney Int. 66 (6) (2004) 2202–2213.
[19] J.Y. Kim, et al., Pharmacological inhibition of caspase-1 ameliorates cisplatin-induced nephrotoxicity through suppression of apoptosis, oxidative stress, and inflammation in mice, Mediat. Inflamm. 2018 (2018) 6571676.
[20] S.M. Man, T.D. Kanneganti, Converging roles of caspases in inflammasome activation, cell death and innate immunity, Nat. Rev. Immunol. 16 (1) (2016) 7–21.
[21] S.K. Yang, et al., Mitochondria targeted peptide SS-31 prevent on cisplatin-induced acute kidney injury via regulating mitochondrial ROS-NLRP3 pathway, Biomed. Pharmacother. 130 (2020) 110521.
[22] P. Mukhopadhyay, et al., Cannabinoid-2 receptor limits inflammation, oxidative/nitrosative stress, and cell death in nephropathy, Free Radic. Biol. Med. 48 (3) (2010) 457–467.
[23] V.V. Giridharan, et al., Schisandrin B, attenuates cisplatin-induced oxidative stress, genotoxicity and neurotoxicity through modulating NF-kappaB pathway in mice, Free Radic. Res. 46 (1) (2012) 50–60.
[24] S. Jamesdaniel, R. Rathinam, W.L. Neumann, Targeting nitrative stress for attenuating cisplatin-induced downregulation of cochlear LIM domain only 4 and ototoxicity, Redox Biol. 10 (2016) 257–265.
[25] G.S. Chiu, et al., Pifithrin-mu prevents cisplatin-induced Chemobrain by preserving neuronal mitochondrial function, Cancer Res. 77 (3) (2017) 742–752.
[26] C. Tan, et al., Endothelium-derived semaphorin 3G regulates hippocampal synaptic Structure and Plasticity via neuropilin-2/PlexinA4, Neuron 101 (5) (2019) 920–937.
[27] M.J. Krashes, et al., Rapid, reversible activation of AgRP neurons drives feeding behavior in mice, J. Clin. Invest. 121 (4) (2011) 1424–1428.
[28] G. Yu, et al., clusterProfiler: an R package for comparing biological themes among gene clusters, OMICS 16 (5) (2012) 284–287.
[29] A. Subramanian, et al., Gene set enrichment analysis: a knowledge-based approach for interpreting genome-wide expression profiles, Proc. Natl. Acad. Sci. U. S. A. 102 (43) (2005) 15545–15550.
[30] X. Li, et al., Visualizing peroxynitrite fluxes in endothelial cells reveals the dynamic progression of brain vascular injury, J. Am. Chem. Soc. 137 (38) (2015) 12296–12303.
[31] X. Xu, et al., One-electron reduction triggered nitric oxide release for ischemia-reperfusion protection, Free Radic. Biol. Med. 164 (2021) 13–19.
[32] M. Sun, et al., Role of pericyte-derived SENP1 in neuronal injury after brain ischemia, CNS Neurosci. Ther. 26 (8) (2020) 815–828.
[33] O. Jensen, L.L. Colgin, Cross-frequency coupling between neuronal oscillations, Trends Cognit. Sci. 11 (7) (2007) 267–269.
[34] R.T. Canolty, R.T. Knight, The functional role of cross-frequency coupling, Trends Cognit. Sci. 14 (11) (2010) 506–515.
[35] K. Nakajima, et al., Gs-coupled GPCR signalling in AgRP neurons triggers sustained increase in food intake, Nat. Commun. 7 (2016) 10268.
[36] M.M. Ollmann, et al., Antagonism of central melanocortin receptors in vitro and in vivo by agouti-related protein, Science 278 (5335) (1997) 135–138.
[37] M.A. Cowley, et al., Integration of NPY, AGRP, and melanocortin signals in the hypothalamic paraventricular nucleus: evidence of a cellular basis for the adipostat, Neuron 24 (1) (1999) 155–163.
[38] V.A. Rathinam, K.A. Fitzgerald, Inflammasome complexes: emerging mechanisms and effector functions, Cell 165 (4) (2016) 792–800.
[39] R.R. Tao, et al., Nitrosative stress induces peroxiredoxin 1 ubiquitination during ischemic insult via E6AP activation in endothelial cells both in vitro and in vivo, Antioxidants Redox Signal. 21 (1) (2014) 1–16.
[40] S. Jin, et al., Drp1 is required for AgRP neuronal activity and feeding, Elife 10 (2021), e64351.
[41] M. Carus-Cadavieco, et al., Gamma oscillations organize top-down signalling to hypothalamus and enable food seeking, Nature 542 (7640) (2017) 232–236.
[42] J. Fell, N. Axmacher, The role of phase synchronization in memory processes, Nat. Rev. Neurosci. 12 (2) (2011) 105–118.
[43] R. Scheffer-Teixeira, A.B. Tort, On cross-frequency phase-phase coupling between theta and gamma oscillations in the hippocampus, Elife 5 (2016) e20515.
[44] M.A. Belluscio, et al., Cross-frequency phase-phase coupling between theta and gamma oscillations in the hippocampus, J. Neurosci. 32 (2) (2012) 423–435.
[45] H. Yan, et al., Cisplatin induces pyroptosis via activation of MEG3/NLRP3/caspase-1/GSDMD pathway in triple-negative breast cancer, Int. J. Biol. Sci. 17 (10) (2021) 2606–2621.
[46] S. Sheth, et al., Mechanisms of cisplatin-induced Ototoxicity and otoprotection, Front. Cell. Neurosci. 11 (2017) 338.
[47] Y. Aponte, D. Atasoy, S.M. Sternson, AGRP neurons are sufficient to orchestrate feeding behavior rapidly and without training, Nat. Neurosci. 14 (3) (2011) 351–355.

[48] C. Zhan, et al., Acute and long-term suppression of feeding behavior by POMC neurons in the brainstem and hypothalamus, respectively, J. Neurosci. 33 (8) (2013) 3624–3632.
[49] D. Atasoy, et al., Deconstruction of a neural circuit for hunger, Nature 488 (7410) (2012) 172–177.
[50] K. Ziegler, et al., Chemical modification of pro-inflammatory proteins by peroxynitrite increases activation of TLR4 and NF-kappaB: implications for the health effects of air pollution and oxidative stress, Redox Biol. 37 (2020) 101581.
[51] U. Landmesser, et al., Oxidation of tetrahydrobiopterin leads to uncoupling of endothelial cell nitric oxide synthase in hypertension, J. Clin. Invest. 111 (8) (2003) 1201–1209.
[52] J. Vasquez-Vivar, B. Kalyanaraman, P. Martasek, The role of tetrahydrobiopterin in superoxide generation from eNOS: enzymology and physiological implications, Free Radic. Res. 37 (2) (2003) 121–127.
[53] S. Bartesaghi, R. Radi, Fundamentals on the biochemistry of peroxynitrite and protein tyrosine nitration, Redox Biol. 14 (2018) 618–625.
[54] R. Czarnomysy, et al., Platinum and palladium complexes as promising sources for antitumor treatments, Int. J. Mol. Sci. 22 (15) (2021).